This article has been accepted for publication in IEEE Internet of Things Journal. This is the author's version which has not been fully edited and content may change prior to final publication. Citation information: DOI 10.1109/JIOT.2022.3224533

Resource Scheduling for Intelligent Reflecting Surface-assisted Full-duplex Wireless Powered Communication Networks with Phase Errors

Sun Mao, Lei Liu, Ning Zhang, Jie Hu, Kun Yang, Mianxiong Dong, and Kaoru Ota

***Abstract*—Intelligent reflecting surface (IRS) is envisioned as a promising technique to improve the performance of full-duplex wireless powered communication networks (FD-WPCNs). This paper investigates the joint phase beamforming design and resource management for IRS-assisted FD-WPCNs, where multiple wireless devices (WDs) can harvest downlink radio-frequency energy and transmit uplink information to the hybrid access point (HAP) over the same band with the aid of IRS. We first formulate a total transmission time minimization problem subject to the minimum transmit rate and energy causality constraints of WDs. In particular, the random phase error of IRS is integrated into our optimization model. Furthermore, we develop an alternating optimization method to obtain the optimal solution of formulated non-convex problem by iteratively solving two subproblems. For the phase beamforming optimization subproblem, we first convert the random phase errors to a deterministic expression, and then utilize the successive convex approximation method to solve the phase beamforming optimization problem. For the transmit power and time-slot allocation subproblem, the optimal transmit power of WDs is derived in closed-form expressions, and the approximation method and variable substitution technique are adopted to obtain the optimal time-slot allocation and transmit power of HAP. Finally, numerical results are provided to evaluate the performance of our proposed method, and reveal the benefits introduced by the IRS technique as compared to benchmark methods.**

***Index Terms*—Intelligent reflecting surface, wireless powered communication networks, full duplex, phase shift errors.**

This work is supported in part by the Natural Science Foundation of Sichuan Province under Grant 2022NSFSC0479, by the Natural Science Foundation of China under Grant 62132004, by the Sichuan Science and Technology Program under Grant 2022YFH0022, by the Sichuan Major R&D Project under Grant 22QYCX0168, by the Guangdong Basic and Applied Basic Research Foundation under Grant 2020A1515110079, by the China Postdoctoral Science Foundation under Grant 2021M692501, by the Fundamental Research Funds for the Central Universities under Grant XJS210107, by the Key Laboratory of Embedded System and Service Computing (Tongji University), by the JSPS KAKENHI under Grants JP19K20250, JP20H04174, and JP22K11989, by the Leading Initiative for Excellent Young Researchers (LEADER), MEXT, Japan, by the JST, PRESTO under Grant JPMJPR21P3, Japan. *(Corresponding author: Lei Liu).*

Sun Mao is with the College of Computer Science, Sichuan Normal University, Chengdu, 610101, China. (E-mail: sunmao@sicnu.edu.cn).

Lei Liu is with the State Key Laboratory of Integrated Service Networks, Xidian University, Xian 710071, China (E-mail: tianjiaoliulei@163.com).

Ning Zhang is with the Department of Electrical and Computer Engineering, University of Windsor, ON, N9B 3P4, Canada (E-mail: ning.zhang@ieee.org).

Jie Hu is with the School of Information and Communication Engineering, University of Electronic Science and Technology of China, Chengdu 611731, China, and also with the Yangtze Delta Region Institute (Huzhou), University of Electronic Science and Technology of China, Huzhou 313001, P. R. China (E-mail: hujie@uestc.edu.cn).

Kun Yang is with School of Computer Technology and Engineering, Changchun Institute of Technology, Changchun 130012, China, and also with School of Information and Communication Engineering, University of Electronic Science and Technology of China, Chengdu 611731, China. (E-mail: kyang@ieee.org).

Mianxiong Dong is with the Department of Sciences and Informatics, Muroran Institute of Technology, Muroran 050-8585, Japan (E-mail: mx.dong@csse.muroran-it.ac.jp).

Kaoru Ota is with the Department of Information and Electronic Engineering, Muroran Institute of Technology, Muroran 050-8585, Japan (E-mail: ota@csse.muroran-it.ac.jp).

I. INTRODUCTION

Internet of things (IoT) has been proposed as a novel paradigm to accommodate massive connectivity for a large number of low-power wireless devices (WDs), e.g., sensors, wearable devices, and so on [1]–[3]. In general, the limited battery capability of WDs is the main bottleneck for the deployment of various IoT applications, such as smart health-care, forest fire monitoring, automatic manufacturing, etc [4]. Therefore, it is crucial to extend the lifetime of WDs in a low-cost manner [5]. Wireless powered communication network (WPCN) is thus proposed as an efficient solution to overcome this bottleneck [6]–[8], where the WDs are able to harvest radio-frequency energy from the HAP, and further transmit the uplink information to the HAP by utilizing the harvested energy. Due to the high pathloss of wireless energy transfer, full-duplex technique has been integrated into WPCNs for extending the energy transfer time and increasing the amount of energy harvested by WDs [9].

Meanwhile, intelligent reflecting surface (IRS) has been proposed as an innovative technique to achieve smart and re-configurable wireless communications in the sixth-generation (6G) era [10]–[15]. In general, IRS is composed by massive passive/active reflection elements, and their amplitudes and phase shifts can be adjusted to enhance the signal strength at intended receivers. Therefore, IRS has great potential to improve the efficiency of wireless energy/information trans-missions in WPCNs. Motivated by these observations, this paper studies the optimal design for IRS-assisted full-duplex WPCNs.

A. Related Works

In this subsection, we will review the existing works from three aspects: (1) Resource Allocation for WPCNs; (2) Full-duplex enhanced WPCNs; (3) IRS-assisted WPCNs.

This article has been accepted for publication in IEEE Internet of Things Journal. This is the author's version which has not been fully edited and content may change prior to final publication. Citation information: DOI 10.1109/JIOT.2022.3224533

1) Resource Allocation for WPCNs: Wireless powered communication network is recognized as a key technique to support sustainable communications in 6G era [16]. Due to the coupled energy and information transmissions, resource allocation plays an important role in improving the performance of WPCNs [17]. In [18], the authors first proposed a "Harvest-then-Transmit" protocol to balance downlink energy transfer and uplink information reception at the HAP, and they maximized the system throughput by proposing a resource allocation strategy. Wu *et al.* in [19] investigated the joint time allocation and power control method to maximize the system energy efficiency of WPCNs. In [20], Lee *et al.* focused on maximizing the total uplink rate for WPCNs considering finite energy storage. In [21], Xiong *et al.* studied the user cooperation strategy for achieving "Win-Win" resource sharing in WPCNs. In [22], the authors presented the robust resource management strategy for WPCNs with non-linear energy harvesting model and imperfect channel state information. To improve the performance of WPCNs, Xie *et al.* in [23] proposed an unmanned aerial vehicle (UAV)-assisted WPCN, where the UAV serves as a flying access point to provide energy/information transmission services for ground wireless devices.

2) Full-duplex enhanced WPCNs: In-band full duplex technique has been envisioned as a promising solution to improve the spectrum efficiency of wireless networks [24]. In recent years, some research works proposed to utilize the full-duplex technique to improve the efficiency of energy/information transmissions in WPCNs. In [25], Ju *et al.* first investigated the resource allocation method for full-duplex W-PCNs, where the HAP is able to transmit the downlink energy signals and receive uplink information signals simultaneously. In [26], Kang *et al.* presented resource management strategies for maximizing the throughput and minimize the transmission latency in full-duplex assisted WPCNs, considering the energy causality constraints. In [27], the authors concentrated on maximizing the secrecy rate for full duplex-assisted WPCNs with multiple potential eavesdroppers. In [28], [29], Iqbal *et al.* formulated the minimum length scheduling problem via jointly optimizing the transmit power and time allocation for full-duplex WPCNs. The authors in [30] investigated the joint beamforming and resource allocation strategy for full-duplex WPCNs, in which the HAP is equipped with multiple antennas for improving the efficiency of energy transfer and information reception.

3) IRS-assisted WPCNs: In recent years, IRS has attracted extensive attention from academia due to its ability to reconstruct wireless propagation environments in a low-cost manner. Therefore, IRS has great potential to improve the performance of WPCNs [31], [32]. Wu *et al.* in [33] first introduced the IRS into WPCNs for improving the efficiency of wireless energy and information transmissions. In [34], the authors focused on maximizing the system throughput for IRS-assisted WPCNs. Due to the hardware restriction and finite resolution of IRS, the adjustable phase shift of IRS is generally discrete. Different from the existing works considering continuous phase shifts, Chu *et al.* in [35] investigated the joint wireless resource and discrete phase shift optimization problem for IRS-assisted WPCNs. Xu *et al.* in [36] focused on the energy efficiency maximization problem for an IRS-assisted multi-antenna WPCNs. In [37], Li *et al.* presented a robust beamforming and resource allocation method for IRS-assisted WPCNs by taking account of the imperfect channel state information. In [38], Lyu *et al.* investigated the optimal design for self-sustainable IRS-assisted WPCNs, where the IRS first harvests energy from downlink energy signals, and then utilizes its reflection link gain to improve the efficiency of energy/information transmissions between HAP and IoT devices. To improve the spectral efficiency, Hua *et al.* in [39] integrated the full-diplex technique into IRS-assisted WPCNs, and they further studied the joint phase beamforming and resource scheduling strategy to maximize the system throughput.

Above works generally considered an ideal scenario without hardware impairments at IRS, which is an unrealistic assumption due to harmful noises, quantization errors, etc. In recent year, some research literature investigated the robust optimization strategy for IRS-assisted communication systems [40], [41]. In [40], Li *et al.* analyzed the ergodic capacity for IRS-assisted communication systems with phase errors, and they modelled the phase error as a random variable that follows uniform distribution at the interval $(-\frac{\pi}{2}, \frac{\pi}{2})$. Chu *et al.* in [41] revealed the impact of transceiver hardware impairments and phase errors of IRS on the throughput performance for IRS-assisted WPCNs.

To sum up, the resource allocation problems for WPCNs have been extensively studied in existing literatures [18]–[23]. Besides, IRS and full-duplex technique were also exploited to improve the efficiency of information and energy transmissions [24]–[39]. Nevertheless, the following issues need to be further addressed:

- Existing works generally focused on the optimization of sum transmission rate or energy efficiency for IRS-assisted WPCNs. The total transmission time is another vital performance indicator, especially in the time-critical applications, such as emergency alert networks. In the literature, it lacks of study to minimize the total transmission time for IRS-assisted WPCNs.
- The full-duplex technique were seldom used to reduce the total transmission time for IRS-assisted WPCNs. Due to the simultaneous energy and information transmissions introduced by full-duplex technique, thus it is a promising solution to reduce the total transmission time by integrating the full-duplex technique into IRS-assisted WPCNs. However, it is difficult to tackle the residual self-interference signals and highly coupled optimization variables in the resource allocation problem for IRS-assisted full-duplex WPCNs.
- In practical IRS-assisted networks, the phase errors of IRS will make a negative impact on the network performance. However, existing works generally assume the perfect phase shift model. Hence, it is essential to optimize the performance of IRS-assisted full-duplex WPCNs considering the practical phase errors at the IRS.

B. Novelty and Contribution

To fill in the gap in existing works, this paper investigates the joint resource allocation and reflection optimization method for IRS-aided full-duplex WPCNs with phase errors. The contribution of this paper is outlined as follows.

- We formulate a total transmission time minimization problem subject to the transmission rate and energy causality constraints of WDs, to jointly optimize time-slot allocation, transmit power control of wireless devices and HAP, and phase beamforming of IRS. Different from the existing works, the phase error of IRS is considered in the formulated problem, and it is modelled as a random variable that follows the uniform distribution.
- To address the formulated non-convex and non-linear optimization problem, we further develop an alternating optimization method to iteratively solve two subproblems. For the phase beamforming optimization subproblem, we first transform the stochastic phase errors to a deterministic form, and then utilize the success convex approximation technique to design an iterative optimization algorithm for obtaining the optimal phase shift matrix of IRS. For the time-slot allocation and transmission power control subproblem, we first derive the closed-form solution for the optimal transmission power of WDs, and further design an iterative algorithm to obtain the optimal time-slot allocation and transmit power of HAP by exploiting the variable substitution technique and approximation method.
- In simulations, we show that the proposed method can realize significantly lower total completion time than the *Without IRS* scheme and *Random phase shift* scheme, which verifies the necessity to deploy IRS with the optimal phase shift design in full-duplex WPCNs. Moreover, we also reveal that the proposed iterative method will converge to the optimal solution within several iterations, and the proposed method with phase errors and energy causality constraints only requires slightly longer transmission time than the *Without energy causality* scheme and *Without phase errors* scheme, which demonstrates the effectiveness of our proposed method.

The remainder of this paper is organized as follows. Section II introduces the system model and transmission protocol for IRS-assisted FD-WPCNs with phase errors. Section III presents the total transmission time minimization problem and the corresponding solution. Section IV illustrates the benchmark methods. Section V provides the simulation results to validate the performance of the proposed method. We conclude this paper in Section VI.

Notations: Hereinafter, lower-case letter, boldface lower-case letter, and boldface upper-case letter stand for scalar, vector and matrix, respectively. For a vector $\mathbf{x}$, $|\mathbf{x}|$, $\mathbf{x}^T$, conj($\mathbf{x}$), $\mathbf{x}^H$ and diag($\mathbf{x}$) denote its module, transpose, conjugate, hermitian transpose and diagonalization, respectively. For a matrix $\mathbf{X}$, Tr($\mathbf{X}$) and Rank($\mathbf{X}$) indicate its trace and rank, respectively. $\mathbb{E}_{\mathbf{x}}(\mathbf{X})$ represents the expectation of $\mathbf{X}$ with respect to the random variable $\mathbf{x}$. $\mathbf{1}_{M\times 1}$ denotes the identity column vector with all elements of 1.

II. System Model

As illustrated in Fig. 1(a), this paper considers an IRS-assisted full-duplex WPCN, consisting of a single-antenna hybrid access point (HAP), an IRS with M reflection elements, and K single-antenna wireless devices (WDs). The sets of reflection units and WDs are indicated by $\mathcal{M} = \{1, 2, \cdots, M\}$ and $\mathcal{K} = \{1, 2, \cdots, K\}$, respectively. In addition, it is assumed that the WDs have no stable energy source and have to harvest radio-frequency (RF) energy from HAP. To improve the spectral efficiency, the HAP works in full-duplex mode for supporting simultaneous uplink information reception and downlink energy transfer over the same band. Moreover, considering the limited size and signal processing capability, the WDs operate in time division duplex mode to avoid harmful co-channel interference. We denote $g_{d,k}$, $\mathbf{g}_r^H \in \mathbb{C}^{1\times M}$ and $\mathbf{g}_{I,k} \in \mathbb{C}^{M\times 1}$ as the uplink channels from the k-th WD to the HAP, from the IRS to the HAP, and from the k-th WD to the IRS, respectively. Besides, the counterpart downlink channels are represented as $h_{d,k}$, $\mathbf{h}_r \in \mathbb{C}^{M\times 1}$ and $\mathbf{h}_{I,k}^H \in \mathbb{C}^{1\times M}$, respectively. It is assumed that all the considered channels follow block-based flat fading, i.e., the channel coefficient keeps fixed during the current time block but may change at the boundaries of time blocks. To reveal the lower bound of total transmission time, the perfect channel state information (CSI) can be obtained at the HAP. In general, the direct channels between the HAP and WDs can be estimated via traditional methods by setting the IRS into the absorbing state. Besides, we can measure the CSI of cascade links between the IRS and HAP/WDs by equipping a small number of low-power radio-frequency chains [42]. The main symbols used in this paper are illustrated in Table I for reference.

The transmission protocol is illustrated in Fig. 1(b), where the first time slot is dedicated for downlink RF energy transfer, while the other time slots are used for both uplink information transmission and downlink energy transfer at the same band simultaneously. In particular, this paper considers the energy causality constraints of WDs, i.e., the k-th WD can only utilize the harvested energy before τ_k to transmit its information to the HAP. Therefore, the available energy of k-th WD is expressed as

$$E_{H,k} = \eta_k \sum_{i=0}^{k-1} \tau_i P_{A,i} |\mathbf{h}_{I,k}^H \hat{\Gamma}_i \mathbf{h}_r + h_{d,k}|^2, \forall k \in \mathcal{K}, \qquad (1)$$

where $\eta_k \in (0, 1]$ denotes the linear energy conversion efficiency, $P_{A,i}$ stands for the downlink transmission power of the HAP during τ_i, and $\hat{\Gamma}_i = \text{diag}\{e^{j(\theta_{i,1}+\theta_{E,i,1})}, e^{j(\theta_{i,2}+\theta_{E,i,2})}, \cdots, e^{j(\theta_{i,M}+\theta_{E,i,M})}\}$ represents the actual phase beamforming matrix of the IRS during τ_i, where $\theta_{i,m}$ and $\theta_{E,i,m}$ denote the phase shift[1]

[1]This paper assumes that the phase shift of IRS can be arbitrarily chosen from (0 2π], in order to reveal the lower bound of total transmission time for the considered system. In fact, the phase shift of IRS can only be chosen from a given discrete set due to the limited resolution of phases. This paper will provide a guidance for the future work considering discrete phase shifts of IRS.

This article has been accepted for publication in IEEE Internet of Things Journal. This is the author's version which has not been fully edited and content may change prior to final publication. Citation information: DOI 10.1109/JIOT.2022.3224533

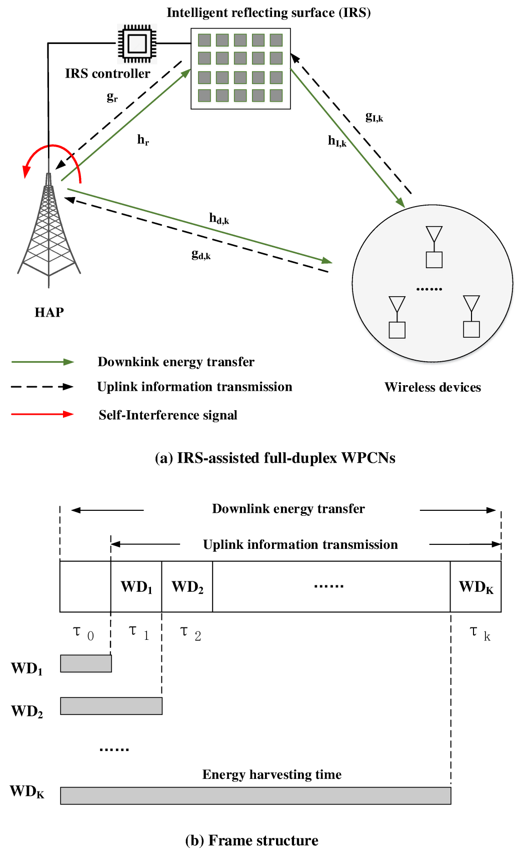

(a) IRS-assisted full-duplex WPCNs

(b) Frame structure

Fig. 1: System Model.

and the additive random phase errors, respectively. Similar to [41], [43], it is assumed that the phase errors follows the uniform distribution, i.e., $\theta_{E,i,m} \sim \mathcal{U}(-\frac{\pi}{2}, \frac{\pi}{2})$. Moreover, this paper considers a linear energy harvesting model, and the method proposed in this work can be directly applied in the scenario with non-linear energy harvesting model. Utilizing the harvested RF energy, the k-th WD will transmit its own information to the HAP during τ_k. Due to the existence of residual self-interference at the HAP, the achievable transmission rate of k-th WD is given by

$$R_k = \tau_k \log_2\left(1 + \frac{P_k|\mathbf{g}_r^H\hat{\Gamma}_k\mathbf{g}_{I,k} + g_{d,k}|^2}{\delta^2 + \gamma P_{A,k}}\right), \forall k \in \mathcal{K}, \quad (2)$$

where P_k denotes the transmission power of the k-th WD, γ is a factor to measure the residual self interference at the HAP, and δ^2 stands for the Gaussian noise power. It should be noted that the interference item generated by the downlink energy signal reflected by IRS is ignored in this paper, since its power is significantly smaller than that of the residual self-interference at the HAP due to the double pathloss [39].

III. Problem Formulation

This work focuses on minimizing the total completion time for downlink energy transfer and uplink information transmissions of all WDs, through joint optimization of time-slot allocation $\{\tau_k, \forall k \in \{0, \mathcal{K}\}\}$, phase beamforming $\{\hat{\Gamma}_k, \forall k \in \{0, \mathcal{K}\}\}$ of the IRS, downlink transmission power $\{P_{A,k}, \forall k \in \{0, \mathcal{K}\}\}$ of HAP, and uplink transmission power $\{P_k, \forall k \in \mathcal{K}\}$ of wireless devices. The total transmission time minimization problem can be formulated as

TABLE I: Summary of major notations

Notation	Description
K	Number of wireless devices
M	Number of reflection units on IRS
$P_{A,k}/P_k$	Transmit power of HAP/k-th wireless device during τ_k
Γ_k	Phase shift matrix of IRS during τ_k
$\Gamma_{E,k}$	Phase error matrix of IRS during τ_k
τ_k	Duration of k-th time slot
δ^2	Gaussian noise power
γ	Self-interference factor
η	Linear energy harvesting efficiency
$R_{k,\min}$	Minimum rate requirement of k-th wireless device
$P_{A,\max}$	Maximum transmit power of HAP
P_u	Path-loss of wireless channel at a unit distance
α	Path-loss factor
M_r	Rician factor of wireless channels

$$\begin{aligned}
&\underset{\{\tau_k,\hat{\Gamma}_k,P_{A,k},P_k\}}{\text{minimize}} \sum_{k=0}^{K} \tau_k \\
&\text{s.t.} \quad \text{C1: } \tau_k \log_2\left(1 + \frac{P_k|\mathbf{g}_r^H\hat{\Gamma}_k\mathbf{g}_{I,k} + g_{d,k}|^2}{\delta^2 + \gamma P_{A,k}}\right) \geq \\
&\qquad\qquad R_{k,\min}, \forall k \in \mathcal{K}, \\
&\qquad \text{C2: } P_k\tau_k \leq \eta_k \sum_{i=0}^{k-1} P_{A,i}\tau_i|\mathbf{h}_{I,k}^H\hat{\Gamma}_i\mathbf{h}_r + h_{d,k}|^2, \\
&\qquad \forall k \in \mathcal{K}, \\
&\qquad \text{C3: } 0 \leq \theta_{k,m} \leq 2\pi, \forall k \in \{0, \mathcal{K}\}, \forall m \in \mathcal{M}, \\
&\qquad \text{C4: } 0 \leq P_{A,k} \leq P_{A,\max}, \forall k \in \{0, \mathcal{K}\}, \\
&\qquad \text{C5: } P_k \geq 0, \tau_k \geq 0, \tau_0 \geq 0, \forall k \in \mathcal{K},
\end{aligned} \quad (3)$$

where C1 implies that the achievable transmission rate of WDs should be larger than their minimum rate requirements, C2 restricts that the communication energy consumption of each WD cannot exceed the harvested RF energy before its transmission time slot, C3 represents the phase shift constraint of reflection elements integrated on the IRS, and C4 restricts the transmit power at the HAP.

As observed, (3) is a non-linear and non-convex optimization problem due to the coupled variables among transmit power, time, and phase beamforming matrix. Moreover, the randomness of phase errors make the problem more difficult to tackle. To deal with this problem, we will design an alternating optimization method to decouple the original problem into two subproblems, i.e., phase beamforming optimization subproblem, and time-slot allocation and transmit power control subproblem. For the phase beamforming subproblem, the random phase error is first transformed to a deterministic form, and then we utilize the successive convex approximation method to obtain the optimal phase shifts of IRS. For the time-slot allocation and transmit power control subproblem, we first derive the optimal transmit power of WDs in closed-form expressions.Then, we rewrite the non-convex transmit rate expression to a more tractable convex form, and design

This article has been accepted for publication in IEEE Internet of Things Journal. This is the author's version which has not been fully edited and content may change prior to final publication. Citation information: DOI 10.1109/JIOT.2022.3224533

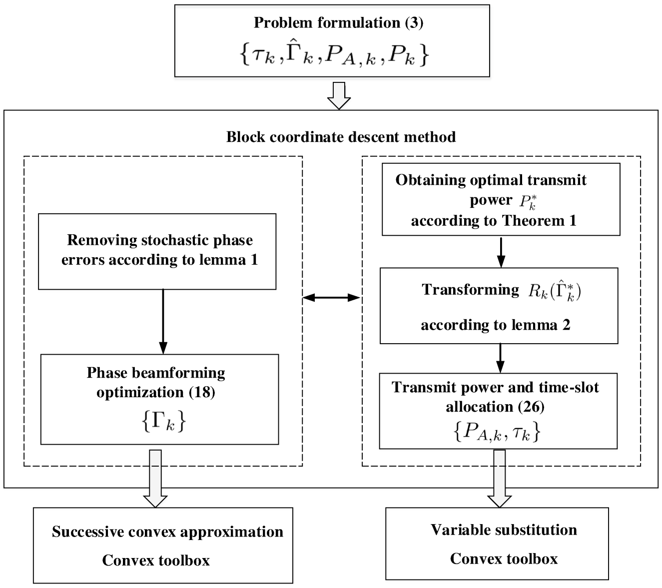

Fig. 2: The flowchart for solving (3).

an iterative method to obtain the optimal time allocation and transmit power control of HAP. The detailed flowchart for solving (3) is illustrated in Fig. 2.

A. Phase Beamforming Optimization Subproblem

Given $\{\tau_k^*, P_{A,k}^*, P_k^*\}$, (3) is simplified to the following phase beamforming optimization subproblem

$$\underset{\{\hat{\Gamma}_k\}}{\text{find}}\ \{\Gamma_k\} \tag{4a}$$

$$\text{s.t.}\ \tau_k^* \log_2\left(1+\frac{P_k^*|\mathbf{g}_r^H\hat{\Gamma}_k\mathbf{g}_{I,k}+g_{d,k}|^2}{\delta^2+\gamma P_{A,k}^*}\right) \geq R_{k,\min}, \forall k \in \mathcal{K}, \tag{4b}$$

$$P_k^*\tau_k^* \leq \eta_k \sum_{i=0}^{k-1} P_{A,i}^*\tau_i^*|\mathbf{h}_{I,k}^H\hat{\Gamma}_i\mathbf{h}_r+h_{d,k}|^2, \forall k \in \mathcal{K}, \tag{4c}$$

$$\text{C3.} \tag{4d}$$

Since $\hat{\Gamma}_k = \Gamma_k\Gamma_{E,k}$ with $\Gamma_k = \text{diag}\{e^{j\theta_{i,1}}, e^{j\theta_{i,2}}, \cdots, e^{j\theta_{i,M}}\}$ and $\Gamma_{E,k} = \text{diag}\{e^{j\theta_{E,i,1}}, e^{j\theta_{E,i,2}}, \cdots, e^{j\theta_{E,i,M}}\}$, we can derive that

$$\begin{aligned} a_k &= |\mathbf{g}_r^H\hat{\Gamma}_k\mathbf{g}_{I,k}+g_{d,k}|^2 \\ &= |\mathbf{g}_r^H\Gamma_k\Gamma_{E,k}\mathbf{g}_{I,k}+g_{d,k}|^2 \\ &= \mathbf{v}_k^H\mathbf{A}_k\text{conj}(\mathbf{v}_{E,k})\mathbf{v}_{E,k}^T\mathbf{A}_k^H\mathbf{v}_k+\mathbf{v}_k^H\mathbf{A}_k\text{conj}(\mathbf{v}_{E,k})g_{d,k}+ \\ &\quad g_{d,k}^H\mathbf{v}_{E,k}^T\mathbf{A}_k^H\mathbf{v}_k+g_{d,k}^Hg_{d,k}, \end{aligned} \tag{5}$$

and

$$\begin{aligned} b_{k,i} &= |\mathbf{h}_{I,k}^H\hat{\Gamma}_i\mathbf{h}_r+h_{d,k}|^2 \\ &= |\mathbf{h}_{I,k}^H\Gamma_i\Gamma_{E,i}\mathbf{h}_r+h_{d,k}|^2 \\ &= \mathbf{v}_i^H\mathbf{B}_k\text{conj}(\mathbf{v}_{E,i})\mathbf{v}_{E,i}^T\mathbf{B}_k^H\mathbf{v}_i+\mathbf{v}_i^H\mathbf{B}_k\text{conj}(\mathbf{v}_{E,i})h_{d,k}+ \\ &\quad h_{d,k}^H\mathbf{v}_{E,i}^T\mathbf{B}_k^H\mathbf{v}_i+h_{d,k}^Hh_{d,k}, \end{aligned} \tag{6}$$

where $\mathbf{v}_k = [e^{j\theta_{k,1}}, \cdots, e^{j\theta_{k,M}}]^T$, $\mathbf{v}_{E,k} = [e^{j\theta_{E,k,1}}, \cdots, e^{j\theta_{E,k,M}}]^T$, $\mathbf{A}_k = \text{diag}(\mathbf{g}_{I,k}^H)\text{diag}(\mathbf{g}_r)$ and $\mathbf{B}_k = \text{diag}(\mathbf{h}_r^H)\text{diag}(\mathbf{h}_{I,k})$. Introducing (5)-(6) into (4), the phase beamforming optimization subproblem will be converted as

$$\underset{\{\mathbf{v}_k\}}{\text{find}}\ \{\mathbf{v}_k\} \tag{7a}$$

$$\text{s.t.}\ \tau_k^* \log_2\left(1+\frac{P_k^*\mathbb{E}_{\mathbf{v}_{E,k}}(a_k)}{\delta^2+\gamma P_{A,k}^*}\right) \geq R_{k,\min}, \forall k \in \mathcal{K}, \tag{7b}$$

$$P_k^*\tau_k^* \leq \eta_k \sum_{i=0}^{k-1} P_{A,i}^*\tau_i^*\mathbb{E}_{\mathbf{v}_{E,i}}(b_{k,i}), \forall k \in \mathcal{K}, \tag{7c}$$

$$\text{C3.} \tag{7d}$$

Due to the randomness of phase errors, we set that the expectation of R_k and $E_{H,k}$ should be larger than $\text{R}_{k,\min}$ and P_kt_k, respectively. In addition, the following lemma is provided o simplify the problem (7).

Lemma 1: $\mathbb{E}_{\mathbf{v}_{E,k}}(a_k)$ and $\mathbb{E}_{\mathbf{v}_{E,i}}(b_{k,i})$ can be rewritten as

$$\begin{aligned} \hat{a}_k &= \mathbb{E}_{\mathbf{v}_{E,k}}(a_k) \\ &= g_{d,k}^Hg_{d,k}+\mathbf{v}_k^H\mathbf{A}_k\mathbb{E}_{\mathbf{v}_{E,k}}\left(\text{conj}(\mathbf{v}_{E,k})\mathbf{v}_{E,k}^T\right)\mathbf{A}_k^H\mathbf{v}_k+ \\ &\quad \mathbf{v}_k^H\mathbf{A}_k\mathbb{E}_{\mathbf{v}_{E,k}}(\text{conj}(\mathbf{v}_{E,k}))g_{d,k}+g_{d,k}^H\mathbb{E}_{\mathbf{v}_{E,k}}(\mathbf{v}_{E,k}^T)\mathbf{A}_k^H\mathbf{v}_k \\ &= g_{d,k}^Hg_{d,k}+\mathbf{v}_k^H\mathbf{A}_k\mathbf{R}\mathbf{A}_k^H\mathbf{v}_k+\frac{2}{\pi}\mathbf{v}_k^H\mathbf{A}_k\mathbf{1}g_{d,k}+ \\ &\quad \frac{2}{\pi}g_{d,k}^H\mathbf{1}^T\mathbf{A}_k^H\mathbf{v}_k, \end{aligned} \tag{8}$$

and

$$\begin{aligned} \hat{b}_{k,i} &= \mathbb{E}_{\mathbf{v}_{E,i}}(b_{k,i}) \\ &= h_{d,k}^Hh_{d,k}+\mathbf{v}_i^H\mathbf{B}_k\mathbb{E}_{\mathbf{v}_{E,i}}\left(\text{conj}(\mathbf{v}_{E,i})\mathbf{v}_{E,i}^T\right)\mathbf{B}_k^H\mathbf{v}_i+ \\ &\quad \mathbf{v}_i^H\mathbf{B}_k\mathbb{E}_{\mathbf{v}_{E,i}}\left(\text{conj}(\mathbf{v}_{E,i})\right)h_{d,k}+h_{d,k}^H\mathbb{E}_{\mathbf{v}_{E,i}}\left(\mathbf{v}_{E,i}^T\right)\mathbf{B}_k^H\mathbf{v}_i \\ &= h_{d,k}^Hh_{d,k}+\mathbf{v}_i^H\mathbf{B}_k\mathbf{R}\mathbf{B}_k^H\mathbf{v}_i+\frac{2}{\pi}\mathbf{v}_i^H\mathbf{B}_k\mathbf{1}h_{d,k}+ \\ &\quad \frac{2}{\pi}h_{d,k}^H\mathbf{1}^T\mathbf{B}_k^H\mathbf{v}_i, \end{aligned} \tag{9}$$

respectively, where

$$\mathbf{R} = \begin{bmatrix} 1 & \frac{4}{\pi^2} & \cdots & \frac{4}{\pi^2} \\ \frac{4}{\pi^2} & 1 & \cdots & \frac{4}{\pi^2} \\ \vdots & \vdots & \ddots & \vdots \\ \frac{4}{\pi^2} & \frac{4}{\pi^2} & \cdots & 1 \end{bmatrix}_{M\times M}. \tag{10}$$

Proof: See Appendix A. ■

According to *Lemma 1*, (7) will be rewritten as

$$\underset{\{\mathbf{v}_k\}}{\text{find}}\ \{\mathbf{v}_k\} \tag{11a}$$

This article has been accepted for publication in IEEE Internet of Things Journal. This is the author's version which has not been fully edited and content may change prior to final publication. Citation information: DOI 10.1109/JIOT.2022.3224533

$$\text{s.t.}\ \tau_k^* \log_2\left(1+\frac{P_k^* \hat{a}_k}{\delta^2+\gamma P_{A,k}^*}\right) \geq R_{k,\min}, \forall k \in \mathcal{K}, \tag{11b}$$

$$P_k^* \tau_k^* \leq \eta_k \sum_{i=0}^{k-1} P_{A,i}^* \tau_i^* \hat{b}_{k,i}, \forall k \in \mathcal{K}, \tag{11c}$$

$$\text{C3}. \tag{11d}$$

After some matrix transformations, (11) is equivalent to the following problem

$$\underset{\{\hat{\mathbf{v}}_k\}}{\text{find}}\ \{\hat{\mathbf{v}}_k\} \tag{12a}$$

$$\text{s.t.}\ \tau_k^* \log_2\left(1+\frac{P_k^* \hat{\mathbf{v}}_k^H \mathbf{Q}_k \hat{\mathbf{v}}_k}{\delta^2+\gamma P_{A,k}^*}\right) \geq R_{k,\min}, \forall k \in \mathcal{K}, \tag{12b}$$

$$P_k^* \tau_k^* \leq \eta_k \sum_{i=0}^{k-1} P_{A,i}^* \tau_i^* \hat{\mathbf{v}}_i^H \mathbf{Z}_k \hat{\mathbf{v}}_i, \forall k \in \mathcal{K}, \tag{12c}$$

$$[\hat{\mathbf{v}}_k \hat{\mathbf{v}}_k^H]_{mm} = 1, \forall m \in \{\mathcal{M}, M+1\}, \forall k \in \{\mathcal{K}, 0\}, \tag{12d}$$

where $\hat{\mathbf{v}}_k = [\mathbf{v}_k^T, 1]^T$,

$$\mathbf{Q}_k = \begin{bmatrix} \mathbf{A}_k \mathbf{R} \mathbf{A}_k^H & \frac{2}{\pi}\mathbf{A}_k \mathbf{1} g_{d,k} \\ \frac{2}{\pi}(\mathbf{A}_k \mathbf{1} g_{d,k})^H & g_{d,k}^H g_{d,k} \end{bmatrix}, \tag{13}$$

$$\mathbf{Z}_k = \begin{bmatrix} \mathbf{B}_k \mathbf{R} \mathbf{B}_k^H & \frac{2}{\pi}\mathbf{B}_k \mathbf{1} h_{d,k} \\ \frac{2}{\pi}(\mathbf{B}_k \mathbf{1} h_{d,k})^H & h_{d,k}^H h_{d,k} \end{bmatrix}. \tag{14}$$

For the purpose of tackling the non-linear equality constraint (12d), the matrix $\hat{\mathbf{V}}_k = \hat{\mathbf{v}}_k \hat{\mathbf{v}}_k^H$ is introduced to rewrite (12) to the following problem

$$\underset{\{\hat{\mathbf{V}}_k\}}{\text{find}}\ \{\hat{\mathbf{V}}_k\} \tag{15a}$$

$$\text{s.t.}\ \tau_k^* \log_2\left(1+\frac{P_k^* \text{Tr}(\mathbf{Q}_k \hat{\mathbf{V}}_k)}{\delta^2+\gamma P_{A,k}}\right) \geq R_{k,\min}, \forall k \in \mathcal{K}, \tag{15b}$$

$$P_k^* \tau_k^* \leq \eta_k \sum_{i=0}^{k-1} P_{A,i}^* \tau_i^* \text{Tr}(\mathbf{Z}_k \hat{\mathbf{V}}_i), \forall k \in \mathcal{K}, \tag{15c}$$

$$[\hat{\mathbf{V}}_k]_{mm} = 1, \forall m \in \{\mathcal{M}, M+1\}, \forall k \in \{\mathcal{K}, 0\}, \tag{15d}$$

$$\hat{\mathbf{V}}_k \succeq 0, \forall k \in \{\mathcal{K}, 0\}, \tag{15e}$$

$$\text{Rank}(\hat{\mathbf{V}}_k) = 1, \forall k \in \{\mathcal{K}, 0\}. \tag{15f}$$

Then, the non-convex rank-one constraint (15f) will be removed. In general, the trace of semi-definite matrix $\hat{\mathbf{V}}_k$ should be no less than its maximum eigenvalue, namely $\text{Tr}(\hat{\mathbf{V}}_k) \geq \lambda_{\max}(\hat{\mathbf{V}}_k)$, and the equality holds when $\text{Rank}(\hat{\mathbf{V}}_k) = 1$. Hence, we can minimize $\sum_{k=0}^{K} \text{Tr}(\hat{\mathbf{V}}_k) - \lambda_{\max}(\hat{\mathbf{V}}_k)$ in the objective function of (15) and drop the rank-one constraint (15f), to reformulate (15) as

$$\underset{\{\hat{\mathbf{V}}_k\}}{\text{minimize}}\ \sum_{k=0}^{K} (\text{Tr}(\hat{\mathbf{V}}_k) - \lambda_{\max}(\hat{\mathbf{V}}_k)) \tag{16a}$$

$$\text{s.t.}\quad \text{(15b)-(15e)}. \tag{16b}$$

By rewriting the convex eigenvalue function $\lambda_{\max}(\hat{\mathbf{V}}_k)$ as its first Taylor approximation, (16) is transformed as

$$\underset{\{\hat{\mathbf{V}}_k\}}{\text{minimize}}\ \sum_{k=0}^{K} (\text{Tr}(\hat{\mathbf{V}}_k) - \lambda_{\max}(\hat{\mathbf{V}}_k^{(i)}) - (\mathbf{v}_{k,\hat{\max}}^{(i)})^H (\hat{\mathbf{V}}_k - \hat{\mathbf{V}}_k^{(i)}) \mathbf{v}_{k,\hat{\max}}^{(i)}) \tag{17a}$$

$$\text{s.t.}\quad \text{(15b)-(15e)}, \tag{17b}$$

where $\hat{\mathbf{V}}_k^{(i)}$ denotes the optimal $\hat{\mathbf{V}}_k$ in the i-th iteration. After eliminating the constant terms in (17a), (17) is simplified as

$$\underset{\{\hat{\mathbf{V}}_k\}}{\text{minimize}}\ \sum_{k=0}^{K} (\text{Tr}(\hat{\mathbf{V}}_k) - (\mathbf{v}_{k,\hat{\max}}^{(i)})^H \hat{\mathbf{V}}_k \mathbf{v}_{k,\hat{\max}}^{(i)}) \tag{18a}$$

$$\text{s.t.}\quad \text{(15b)-(15e)}. \tag{18b}$$

When $\text{Tr}(\hat{\mathbf{V}}_k) - \lambda_{\max}(\hat{\mathbf{V}}_k) \approx 0$, it means that $\hat{\mathbf{V}}_k \approx \lambda_{\max}(\hat{\mathbf{V}}_k) \mathbf{v}_{k,\hat{\max}} \mathbf{v}_{k,\hat{\max}}^H$, where $\mathbf{v}_{k,\hat{\max}}$ represents the unit eigenvector corresponding to the maximum eigenvalue $\lambda_{\max}(\hat{\mathbf{V}}_k)$. Thus, the optimal beamforming vector $\mathbf{v}_{k,\hat{\max}}$ will be recovered using the following equation:

$$\hat{\mathbf{v}}_k = \sqrt{\lambda_{\max}(\hat{\mathbf{V}}_k)} \mathbf{v}_{k,\hat{\max}}. \tag{19}$$

We summarize the whole procedure for solving (4) in Algorithm 1.

Algorithm 1: SCA-based method for solving the phase beamforming optimization subproblem (4)

---

1 **Initialize:** Set $(\hat{\mathbf{V}}_0^{(0)}, \hat{\mathbf{V}}_1^{(0)}, \cdots, \hat{\mathbf{V}}_K^{(0)})$, $(\mathbf{v}_{0,\hat{\max}}^{(0)}, \mathbf{v}_{1,\hat{\max}}^{(0)}, \cdots, \mathbf{v}_{K,\hat{\max}}^{(0)})$, and $i = 1$.
2 **Repeat:**
3 Solving (18) by utilizing the convex toolbox, such as CVX or Yalmip, to obtain optimal $\{\hat{\mathbf{V}}_k^*\}$;
4 Setting $\hat{\mathbf{V}}_k^{(i)} = \hat{\mathbf{V}}_k^*$;
5 Calculating the maximum eigenvalue $\lambda_{\max}(\hat{\mathbf{V}}_k^{(i)})$ and the corresponding eigenvector $\mathbf{v}_{k,\hat{\max}}^{(i)}$;
6 Updating the iterative number $i = i + 1$;
7 **Until Convergence**.
8 **Return** optimal phase beamforming matrix $\{\hat{\mathbf{V}}_k^{(i)}\}$.

B. Time-Slot Allocation and Transmission Power Control

Under given $\{\hat{\Gamma}_k^*\}$, (3) will be reduced to the following problem

$$\underset{\{\tau_k, P_{A,k}, P_k\}}{\text{minimize}}\ \sum_{k=0}^{K} \tau_k \tag{20a}$$

$$\text{s.t.}\quad \tau_k \log_2\left(1+\frac{P_k |\mathbf{g}_r^H \hat{\Gamma}_k^* \mathbf{g}_{I,k} + g_{d,k}|^2}{\delta^2+\gamma P_{A,k}}\right) \geq R_{k,\min}, \forall k \in \mathcal{K}, \tag{20b}$$

This article has been accepted for publication in IEEE Internet of Things Journal. This is the author's version which has not been fully edited and content may change prior to final publication. Citation information: DOI 10.1109/JIOT.2022.3224533

$$P_k\tau_k \le \eta_k \sum_{i=0}^{k-1} P_{A,i}\tau_i |\mathbf{h}_{I,k}^H \hat{\Gamma}_i^* \mathbf{h}_r + h_{d,k}|^2, \forall k \in \mathcal{K}, \tag{20c}$$

$$0 \le P_{A,k} \le P_{A,\max}, \forall k \in \{0, \mathcal{K}\}, \tag{20d}$$

$$P_k \ge 0, \tau_k \ge 0, \tau_0 \ge 0, \forall k \in \mathcal{K}. \tag{20e}$$

Theorem 1: The minimum completion time is achieved when the WDs exhaust their harvested radio-frequency energy for transmitting information to the HAP, i.e.,

$$P_k^*\tau_k^* = \eta_k \sum_{i=0}^{k-1} P_{A,i}^*\tau_i^* |\mathbf{h}_{I,k}^H \hat{\Gamma}_i^* \mathbf{h}_r + h_{d,k}|^2, \forall k \in \mathcal{K}. \tag{21}$$

Proof: Assuming that $\{\tau_0^+, \tau_k^+, P_{A,k}^+, P_k^+\}$ achieves the minimum total completion time for (20) while there exists a WD j who does not exhaust its harvested energy, i.e., $P_j^+\tau_j^+ < \eta_j \sum_{i=0}^{j-1} P_{A,i}^+\tau_i^+ |\mathbf{h}_{I,j}^H \hat{\Gamma}_i^* \mathbf{h}_r + h_{d,j}|^2$, and $P_k^+\tau_k^+ = \eta_k \sum_{i=0}^{k-1} P_{A,i}^+\tau_i^+ |\mathbf{h}_{I,k}^H \hat{\Gamma}_i^* \mathbf{h}_r + h_{d,k}|^2$ for $k \neq j$. Then, we can construct another solution $\{\tau_0^*, \tau_k^*, P_{A,k}^*, P_k^*\}$ satisfying $\tau_0^* = \tau_0^+$, $\tau_j^* = \beta\tau_j^+$, $\tau_k^* = \tau_k^+$, $P_{A,k}^* = P_{A,k}^+$, $P_j^* = \alpha P_j^+$, and $P_k^* = P_k^+$, where $\alpha > 1$ and $\beta < 1$, which satisfies $\beta\tau_j^+ \log_2\left(1 + \frac{\alpha P_j^+ |\mathbf{g}_r^H \hat{\Gamma}_j^* \mathbf{g}_{I,j} + g_{d,j}|^2}{\delta^2 + \gamma P_{A,j}^*}\right) \ge R_{j,\min}$ and $\alpha\beta P_j^+\tau_j^+ \le \eta_j \sum_{i=0}^{j-1} P_{A,i}^*\tau_i^* |\mathbf{h}_{I,j}^H \hat{\Gamma}_i^* \mathbf{h}_r + h_{d,j}|^2$. First, it is easy to verify that $\{\tau_0^*, \tau_k^*, P_{A,k}^*, P_k^*\}$ still satisfies constraints (20b)-(20d), and we have $\sum_{k=0}^{K} \tau_k^* = \beta\tau_j^+ + \sum_{k\neq j} \tau_k^* < \sum_{k=0}^{K} \tau_k^+$, which contradicts with the assumption. *Theorem 1* is thus proved. ■

Based on *Theorem 1*, (20) will be simplified as the following problem

$$\underset{\{\tau_k, P_{A,k}\}}{\text{minimize}} \sum_{k=0}^{K} \tau_k \tag{22a}$$

$$\text{s.t.} \quad \tau_k \log_2\left(1 + \frac{\sum_{i=0}^{k-1} r_{i,k} P_{A,i}\tau_i}{\tau_k(\delta^2 + \gamma P_{A,k})}\right) \ge R_{k,\min}, \forall k \in \mathcal{K}, \tag{22b}$$

$$0 \le P_{A,k} \le P_{A,\max}, \forall k \in \{0, \mathcal{K}\}, \tag{22c}$$

$$\tau_k \ge 0, \tau_0 \ge 0, \forall k \in \mathcal{K}, \tag{22d}$$

where $r_{i,k} = \eta_k |\mathbf{h}_{I,k}^H \hat{\Gamma}_i^* \mathbf{h}_r + h_{d,k}|^2 |\mathbf{g}_r^H \hat{\Gamma}_k^* \mathbf{g}_{I,k} + g_{d,k}|^2$. To decouple the time and power variables, we introduce a set of auxiliary variables $\epsilon_{A,k} = P_{A,k}\tau_k$ to reformulate (22) as

$$\underset{\{\tau_k, \epsilon_{A,k}\}}{\text{minimize}} \sum_{k=0}^{K} \tau_k \tag{23a}$$

$$\text{s.t.} \quad \tau_k \log_2\left(1 + \frac{\sum_{i=0}^{k-1} r_{i,k}\epsilon_{A,i}}{\tau_k\delta^2 + \gamma\epsilon_{A,k}}\right) \ge R_{k,\min}, \forall k \in \mathcal{K}, \tag{23b}$$

$$0 \le \epsilon_{A,k} \le \tau_k P_{A,\max}, \forall k \in \{0, \mathcal{K}\}, \tag{23c}$$

$$\tau_k \ge 0, \tau_0 \ge 0, \forall k \in \mathcal{K}, \tag{23d}$$

As observed, (23) is nonconvex due to the constraint (23b). The following *Lemma 2* will be proposed to tackle it.

Lemma 2: Defining $f(y) = -yx + \ln(y) + 1$, we have

$$-\ln x = \max_{y>0} f(y). \tag{24}$$

The equality holds when $y = 1/x$. Defining $x = \tau_k\delta^2 + \gamma\epsilon_{A,k}$ and $y = y_k^{(i)}$, $R_k(\hat{\Gamma}_k^*)/\tau_k$ can be rewritten as

$$\begin{aligned}\frac{R_k(\hat{\Gamma}_k^*)}{\tau_k} &= \log_2\left(1 + \frac{\sum_{i=0}^{k-1} r_{i,k}\epsilon_{A,i}}{\tau_k\delta^2 + \gamma\epsilon_{A,k}}\right)\\
&= \frac{1}{\ln 2}(\ln(\tau_k\delta^2 + \gamma\epsilon_{A,k} + \sum_{i=0}^{k-1} r_{i,k}\epsilon_{A,i}) - \ln(\tau_k\delta^2 + \gamma\epsilon_{A,k}))\\
&= \frac{1}{\ln 2}(\ln(\tau_k\delta^2 + \gamma\epsilon_{A,k} + \sum_{i=0}^{k-1} r_{i,k}\epsilon_{A,i}) - y_k^{(i)}(\tau_k\delta^2 + \gamma\epsilon_{A,k})\\
&\quad + \ln(y_k^{(i)}) + 1).\end{aligned} \tag{25}$$

Therefore, (23) will be converted as

$$\underset{\{\tau_k, \epsilon_{A,k}\}}{\text{minimize}} \sum_{k=0}^{K} \tau_k \tag{26a}$$

$$\begin{aligned}\text{s.t.} \quad &\frac{1}{\ln 2}(\ln(\tau_k\delta^2 + \gamma\epsilon_{A,k} + \sum_{i=0}^{k-1} r_{i,k}\epsilon_{A,i}) - y_k^{(i)}(\tau_k\delta^2 +\\
&\gamma\epsilon_{A,k}) + \ln(y_k^{(i)}) + 1) \ge \frac{R_{k,\min}}{\tau_k}, \forall k \in \mathcal{K},\end{aligned} \tag{26b}$$

$$\text{(23c)-(23d).} \tag{26c}$$

Theorem 2: The time allocation and transmit power control subproblem (26) is a convex optimization problem.

Proof: $\ln(\tau_k\delta^2 + \gamma\epsilon_{A,k} + \sum_{i=0}^{k-1} r_{i,k}\epsilon_{A,i})$ is a concave function with respect to $\{\tau_k, \epsilon_k\}$. In addition $\frac{R_{k,\min}}{\tau_k}$ is a convex function of τ_k. Therefore, (26b) is the typical convex constraint. Integrated with the linear objective function and constraints, we will prove that (26) is convex. ■

Therefore, we can adopt some convex optimization toolboxes to solve (26). The detailed procedure for solving (20) is illustrated in the following Algorithm 2.

C. Algorithm Procedure and Complexity Analysis

In summary, the alternating optimization method for solving the total completion time minimization problem (3) is presented in Algorithm 3.

This article has been accepted for publication in IEEE Internet of Things Journal. This is the author's version which has not been fully edited and content may change prior to final publication. Citation information: DOI 10.1109/JIOT.2022.3224533

Algorithm 2: Proposed method for solving time-slot allocation and power control problem (20)

1 **Initialize:** Set $\{\tau_k^{(0)}, P_{A,k}^{(0)}, P_k^{(0)}\}$, and $i = 1$.
2 **Repeat:**
3 Computing $P_k^{(i)}$ according to (21);
4 Calculating $y_k^{(i)} = \frac{1}{\tau_k^{(i-1)}\delta^2 + \gamma \tau_k^{(i-1)} P_{A,k}^{(i-1)}}$;
5 Acquiring the optimal $\{\tau_k^{(i)}, \epsilon_k^{(i)}\}$ by solving (26);
6 Computing $P_{A,k}^{(i)} = \frac{\epsilon_k^{(i)}}{\tau_k^{(i)}}$;
7 Updating the iteration factor $i = i + 1$;
8 **Until** convergence.
9 **Obtaining** optimal solution $\{\tau_k^*, P_{A,k}^*, P_k^*\}$.

Algorithm 3: Alternating optimization method for solving the total completion time minimization problem (3)

1 **Initialize:** Set $(\tau_k^{(0)}, P_{A,k}^{(0)}, P_k^{(0)}, \hat{\mathbf{V}}_k{}^{(0)})$, and $n = 1$.
2 **Repeat:**
3 Adopting Algorithm 1 to obtain the optimal phase beamforming matrix $\{\hat{\mathbf{V}}_k{}^{(n)}\}$,
4 Computing the optimal time-slot allocation and power control strategy $\{\tau_k^{(n)}, P_{A,k}^{(n)}, P_k^{(n)}\}$ by executing Algorithm 2;
5 Updating the iteration factor $n = n + 1$;
6 **Until** convergence.
7 **Return:** $(\tau_k^*, P_{A,k}^*, P_k^*, \hat{\mathbf{V}}_k{}^*)$=$(\tau_k^{(n)}, P_{A,k}^{(n)}, P_k^{(n)}, \hat{\mathbf{V}}_k{}^{(n)})$.

Theorem 3: Algorithm 3 can converge to the optimal solution after several iterations.

Proof: Denoting $T_{\text{tot}}(\tau_k, P_{A,k}, P_k, \hat{\mathbf{V}}_k)$ as the objective function of (3) and n as the iteration index, we will prove the convergence of Algorithm 3 as follows. In the step 3 of Algorithm 3, since $\{\hat{\mathbf{V}}_k^{(n+1)}\}$ is the suboptimal phase beamforming strategy under given $\{\tau_k^{(n)}, P_{A,k}^{(n)}, P_k^{(n)}\}$, we have

$$T_{\text{tot}}(\tau_k^{(n)}, P_{A,k}^{(n)}, P_k^{(n)}, \hat{\mathbf{V}}_k^{(n)}) \geq T_{\text{tot}}(\tau_k^{(n)}, P_{A,k}^{(n)}, P_k^{(n)}, \hat{\mathbf{V}}_k^{(n+1)}). \tag{27}$$

In the step 4 of Algorithm 3, given $\{\hat{\mathbf{V}}_k^{(n+1)}\}$, $\{\tau_k^{(n+1)}, P_{A,k}^{(n+1)}, P_k^{(n+1)}\}$ is the suboptimal time-slot allocation and transmit power control scheme of (20), which satisfies

$$\begin{aligned} &T_{\text{tot}}(\tau_k^{(n)}, P_{A,k}^{(n)}, P_k^{(n)}, \hat{\mathbf{V}}_k^{(n+1)}) \geq \\ &T_{\text{tot}}(\tau_k^{(n+1)}, P_{A,k}^{(n+1)}, P_k^{(n+1)}, \hat{\mathbf{V}}_k^{(n+1)}). \end{aligned} \tag{28}$$

Hence, $T_{\text{tot}}(\tau_k, P_{A,k}, P_k, \hat{\mathbf{V}}_k)$ is non-increasing versus the iteration index. Besides, the total transmission time is limited. According to Cauchy theory, we derive that Algorithm 3 will coverage to an optimal value after a finite number of iterations [44]. ■

Next, we will analyze the computational complexity of Algorithm 3. Suppose I_1, I_2 and I_3 are the iteration number of Algorithm 1 and Algorithm 2, and Algorithm 3, respectively. In each iteration, the computational complexity of Algorithm 3 mainly includes the complexity for solving two subproblems.

- For the phase beamforming optimization subproblem, the complexity for solving convex problem (18) will be $\mathcal{O}((3K+1+K(M+1)^2+(K+1)(M+1))(K(M+1)^2)^2\sqrt{3K+1+(K+1)(M+1)}\log(1/\epsilon_1))$ with $K(M+1)^2$ variables and $3K+1+(K+1)(M+1)$ constraints, where ϵ_1 denotes the tolerance factor for solving (18). In addition, the complexity for calculating eigenvalues and eigenvectors of $\{\hat{\mathbf{V}}_k\}$ will be $\mathcal{O}((K+1)(M+1)^3)$. Therefore, the total complexity of Algorithm 1 is given by $\mathcal{O}(I_1((3K+1+K(M+1)^2+(K+1)(M+1))(K(M+1)^2)^2\sqrt{3K+1+(K+1)(M+1)}\log(1/\epsilon_1)+(K+1)(M+1)^3))$.
- For the time-slot allocation and transmit power control subproblem, the complexity for solving (26) can be calculated as $\mathcal{O}(4(5K+4)(K+1)^2\sqrt{3K+2}\log(1/\epsilon_2))$ with $2(K+1)$ constraints and $3K+2$ constraints, where ϵ_2 stands for the tolerance factor for solving (26). The total complexity for Algorithm 2 is given by $\mathcal{O}(I_2(4(5K+4)(K+1)^2\sqrt{3K+2}\log(1/\epsilon_2)))$.

In summary, the complexity of Algorithm 3 is $\mathcal{O}(I_3(I_1((3K+1+K(M+1)^2+(K+1)(M+1))(K(M+1)^2)^2\sqrt{3K+1+(K+1)(M+1)}\log(1/\epsilon_1)+(K+1)(M+1)^3)+I_2(4(5K+4)(K+1)^2\sqrt{3K+2}\log(1/\epsilon_2))))$.

IV. Simulation Results

This section illustrates the simulation results to validate the superiority of the proposed approach in terms of the total transmission time for IRS-assisted full-duplex WPCNs, as compared to several benchmark methods, i.e., *Without phase errors* scheme, *Without IRS* scheme, *Without energy causality* scheme, and *Random phase shift* scheme. It should be noted that the benchmark methods are illustrated in Appendix B. The simulation parameters are set as follows: $M = 60$, $K = 2$, $\delta^2 = 10^{-9}$ W, $\eta_k = 0.8$, $\gamma = 10^{-12}$, $P_{A,k} = 5$ W, and $R_{k,\min} = 0.1$ bits/Hz. The coordinations of HAP, IRS, and WDs are [0, 0], [0, 3], and ([2, 3], [1, 4]), respectively. In simulations, the channel coefficient is modeled as

$$\mathbf{C_h} = \sqrt{P_u d^{-\alpha}}\left(\sqrt{\frac{M_r}{M_r+1}}\mathbf{C}_r^{\text{LoS}} + \sqrt{\frac{1}{M_r+1}}\mathbf{C}_r^{\text{NLoS}}\right), \tag{29}$$

where $P_u = 10^{-2}$ is the path-loss of unit distance, d stands for the distance among communication nodes, $\alpha = 2$ represents the path-loss factor, $M_r = 3$ denotes the Rician factor, and $\mathbf{C}_r^{\text{LoS}}$ and $\mathbf{C}_r^{\text{NLoS}}$ indicate the Line-of-Sight (LoS) and Rayleigh fading components, respectively.

In Fig. 3, we illustrate the total completion time against the transmission rate requirements of WDs. As observed, the total transmission time yields an increasing trend with $R_{k,\min}$ for all schemes. This is because that the increase of $R_{k,\min}$ will inevitably lead to extend the information/energy transmission time for satisfying strict transmission rate requirements. Moreover, the proposed method outperforms the *Without IRS* scheme and the *Random phase shift* scheme. This observation

This article has been accepted for publication in IEEE Internet of Things Journal. This is the author's version which has not been fully edited and content may change prior to final publication. Citation information: DOI 10.1109/JIOT.2022.3224533

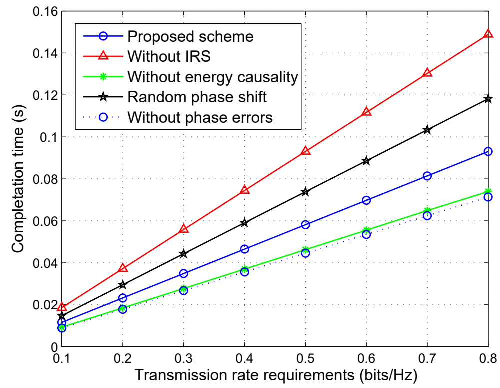

Fig. 3: The total completion time versus transmission rate requirements

confirms that the optimization design of IRS exhibits an important role in reducing the total transmission time for IRS-assisted full-duplex WPCNs. Besides, the perfect case without phase errors provides a lower total completion time compared to the proposed method with phase errors, which means that the phase errors have a negative impact on the system performance.

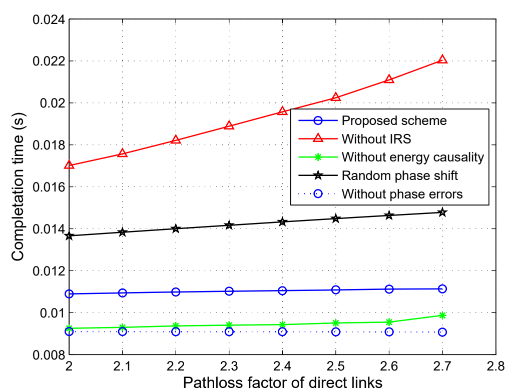

Fig. 4: The total completion time versus path-loss factor of direct links

Fig. 4 shows the relationship between the total completion time and path-loss factor of direct links. From this figure, we find that the total completion time of all schemes exhibits a declining trend with the path-loss factor of direct links. This is due to the fact that more severe channel fading will lead to a lower energy/information transmission efficiency, and it will further result in the increase of total completion time. Meanwhile, the time reduction achieved by the proposed method increases with the path-loss factor of direct links, as compared with the *Without IRS* scheme. Because that the cascade links aided by the IRS become a good choice to improve the efficiency of information/energy transmissions, when the direct links undergo deep fading. In addition, the proposed method with energy causality constraints have a slightly degraded performance than the *Without energy causality* scheme, because the latter method allows the WD to utilize the harvested energy after its uplink transmit slot, and in turn, decreases the information transmission duration.

In Fig. 5, we reveal the impact of the number of reflection elements on the total completion time. From this figure, the total completion time achieved by IRS-assisted schemes has a decreasing tend with the increase of M. Specifically, the time reduction achieved by our proposed method increases with M than both the *Without IRS* scheme and *Random phase shift* scheme. This validates the necessity to optimize the phase beamforming method for IRS-assisted full-duplex WPCNs, especially when the IRS is equipped with a large number of reflection elements.

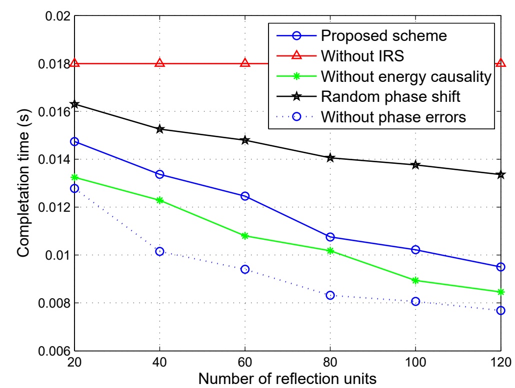

Fig. 5: The total completion time versus number of reflection elements.

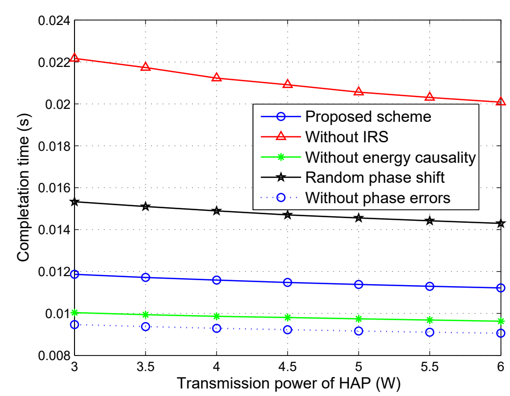

Fig. 6: The total completion time versus maximum transmit power of HAP.

In Fig. 6, we plot the total completion time against the maximum transmit power of HAP. As desired, the total completion time achieved by all schemes decreases with the increase of maximum transmit power at the HAP. Because the energy transmission time will be reduced with a larger transmit power of HAP. Moreover, we also see that the proposed method can realize at least 83% and 29% time reduction than the *Without IRS* scheme and *Random phase shift* scheme, respectively. Meanwhile, it is also shown that the proposed method consumes 20% and 26% more transmission time than the *Without energy causality* scheme and *Without phase*

This article has been accepted for publication in IEEE Internet of Things Journal. This is the author's version which has not been fully edited and content may change prior to final publication. Citation information: DOI 10.1109/JIOT.2022.3224533

errors scheme, respectively. Fig. 7 reveal the convergence rate of Algorithm 3, where one can see that the proposed Algorithm 3 will converge to the optimal solution after several iterations under different parameter settings. It demonstrates the good convergence property of our proposed alternating optimization method.

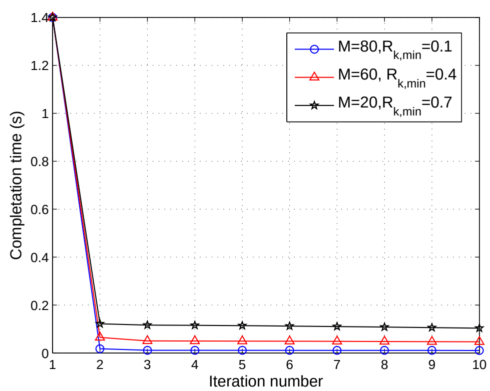

Fig. 7: Convergence rate of Algorithm 3.

V. CONCLUSION

This paper studied the impact of phase errors on the performance of IRS-assisted full-duplex WPCNs in terms of total transmission time. First, we formulated a total completion time minimization problem under the transmit rate and energy causality constraints of WDs, via jointly optimizing the time-slot allocation, phase beamforming of IRS, and transmit power control of WDs and HAP. To solve this problem, we decoupled the original problem into two subproblems by exploiting the block coordinate descent method. For the phase beamforming optimization subproblem, we transformed the random phase errors to a deterministic form, and further designed an iterative method to obtain the optimal phase beamforming strategy by exploiting the successive convex approximation technique. For the time allocation and transmit power control subproblem, we derive the optimal transmit power of WDs in closed-form expressions, and utilized the variable substitution and approximation method to obtain the optimal time allocation and transmit power of HAP. Simulation results demonstrated that the completion time can be greatly reduced by our proposed method, as compared with the *Without IRS* scheme and *Random phase shift* scheme. Besides, we also observed that the proposed method consumed a little more total completion time than the *Without energy causality* scheme and *Without phase errors* scheme.

In the future, we can extend the current work to several interesting research directions. First, active IRS can be considered to improve the performance of full-duplex WPCNs via jointly optimizing phase shifts and amplitudes of reflection elements on IRS. Second, the robust resource management and reflection optimization strategy is able to be designed considering the imperfect CSI and transceiver hardware impairments. Finally, it is meaningful to investigate the optimal design problem for the multi-cell scenario, and meanwhile multiple IRS can be deployed to improve the performance of full-duplex WPCNs.

APPENDIX A: PROOF OF *Lemma 1*

We first derive $\mathbb{E}_{\mathbf{v}_{E,k}}(\text{conj}(\mathbf{v}_{E,k})\mathbf{v}_{E,k}^T)$, $\mathbb{E}_{\mathbf{v}_{E,k}}(\text{conj}(\mathbf{v}_{E,k}))$ and $\mathbb{E}_{\mathbf{v}_{E,k}}(\mathbf{v}_{E,k}^T)$. The expression of $\text{conj}(\mathbf{v}_{E,k})\mathbf{v}_{E,k}^T$ is given by

$$\begin{bmatrix} 1 & e^{j(\theta_{E,k,2}-\theta_{E,k,1})} & \dots & e^{j(\theta_{E,k,M}-\theta_{E,k,1})} \\ e^{j(\theta_{E,k,1}-\theta_{E,k,2})} & 1 & \dots & e^{j(\theta_{E,k,M}-\theta_{E,k,2})} \\ \vdots & \vdots & \ddots & \vdots \\ e^{j(\theta_{E,k,1}-\theta_{E,k,M})} & e^{j(\theta_{E,k,2}-\theta_{E,k,M})} & \dots & 1 \end{bmatrix}. \tag{30}$$

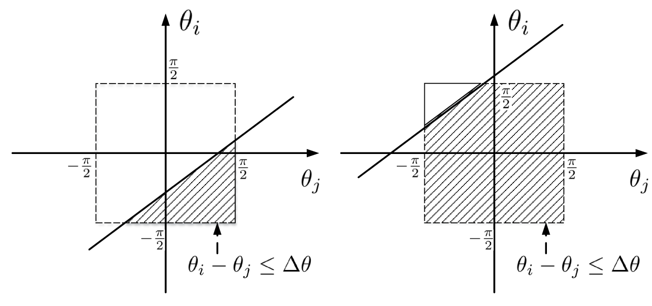

(a) $-\pi \leq \Delta\theta_{i,j} \leq 0$ **(b)** $0 < \Delta\theta_{i,j} \leq \pi$

Fig. 8: The domain of integration for distribution function.

Since $\theta_{E,k,m} \sim \mathcal{U}(-\frac{\pi}{2}, \frac{\pi}{2})$, we will derive the probability density function (PDF) of $\Delta\theta_{i,j} = \theta_{E,k,i} - \theta_{E,k,j}, \forall i \neq j$. It exists the following several cases:

- $|\Delta\theta_{i,j}| > \pi$: it is out of the scope of $\Delta\theta_{i,j}$, so its PDF will be $f_{\Delta\theta_{i,j}}(\Delta\theta) = 0$.
- $-\pi \leq \Delta\theta_{i,j} \leq 0$: According to Fig. 8 (a), the distribution function $F_{\Delta\theta_{i,j}}(\Delta\theta)$ will be

$$\begin{aligned} &F_{\Delta\theta_{i,j}}(\Delta\theta) = \mathbb{P}\{\Delta\theta_{i,j} \leq \Delta\theta\} \\ &= \int_{-\frac{\pi}{2}-\Delta\theta}^{\frac{\pi}{2}} \int_{-\frac{\pi}{2}}^{\theta_j+\Delta\theta} f_{\theta_{E,k,i},\theta_{E,k,j}}(\theta_i,\theta_j) d\theta_i d\theta_j \\ &= \int_{-\frac{\pi}{2}-\Delta\theta}^{\frac{\pi}{2}} \int_{-\frac{\pi}{2}}^{\theta_j+\Delta\theta} f_{\theta_{E,k,i}}(\theta_i) f_{\theta_{E,k,j}}(\theta_j) d\theta_i d\theta_j \\ &= \int_{-\frac{\pi}{2}-\Delta\theta}^{\frac{\pi}{2}} \int_{-\frac{\pi}{2}}^{\theta_j+\Delta\theta} \frac{1}{\pi^2} d\theta_i d\theta_j \\ &= \frac{\Delta\theta^2}{2\pi^2} + \frac{\Delta\theta}{\pi} + \frac{1}{2}. \end{aligned} \tag{31}$$

  Therefore, the PDF of $\Delta\theta_{i,j}$ at the interval $[-\pi, 0]$ is given by

$$f_{\Delta\theta_{i,j}}(\Delta\theta) = \frac{\partial F_{\Delta\theta_{i,j}}(\Delta\theta)}{\partial \Delta\theta} = \frac{\Delta\theta}{\pi^2} + \frac{1}{\pi}. \tag{32}$$

- $0 < \Delta\theta_{i,j} \leq \pi$: By observing Fig. 8(b), the distribution function $F_{\Delta\theta_{i,j}}(\Delta\theta)$ can be expressed as

$$\begin{aligned}
&F_{\Delta\theta_{i,j}}(\Delta\theta) = \mathbb{P}\{\Delta\theta_{i,j} \leq \Delta\theta\} \\
&= \int_{-\frac{\pi}{2}}^{\frac{\pi}{2}-\Delta\theta} \int_{-\frac{\pi}{2}}^{\theta_j+\Delta\theta} f_{\theta_{E,k,i},\theta_{E,k,j}}(\theta_i,\theta_j) d\theta_i d\theta_j \\
&+ \int_{\frac{\pi}{2}-\Delta\theta}^{\frac{\pi}{2}} \int_{-\frac{\pi}{2}}^{\frac{\pi}{2}} f_{\theta_{E,k,i},\theta_{E,k,j}}(\theta_i,\theta_j) d\theta_i d\theta_j \\
&= \frac{1}{2} - \frac{\Delta\theta^2}{2\pi^2} + \frac{\Delta\theta}{\pi}.
\end{aligned} \tag{33}$$

Hence, the PDF of $\Delta\theta_{i,j}$ at the interval $(0,\pi]$ is expressed as

$$f_{\Delta\theta_{i,j}}(\Delta\theta) = \frac{\partial F_{\Delta\theta_{i,j}}(\Delta\theta)}{\partial \Delta\theta} = -\frac{\Delta\theta}{\pi^2} + \frac{1}{\pi}. \tag{34}$$

According to above descriptions, the PDF of $\Delta\theta_{i,j}$ will be

$$f_{\Delta\theta_{i,j}}(\Delta\theta) = \begin{cases} \frac{\Delta\theta}{\pi^2} + \frac{1}{\pi}, & -\pi \leq \Delta\theta \leq 0 \\ -\frac{\Delta\theta}{\pi^2} + \frac{1}{\pi}, & 0 < \Delta\theta \leq \pi \\ 0. & \text{otherwise} \end{cases} \tag{35}$$

Then, $\mathbb{E}_{\Delta\theta_{i,j}}(e^{j\Delta\theta_{i,j}})$ is derived as

$$\begin{aligned}
&\mathbb{E}_{\Delta\theta_{i,j}}(e^{j\Delta\theta_{i,j}}) = \int_{-\pi}^{0} (\frac{\Delta\theta}{\pi^2} + \frac{1}{\pi}) e^{j\Delta\theta} d\Delta\theta \\
&+ \int_{0}^{\pi} (-\frac{\Delta\theta}{\pi^2} + \frac{1}{\pi}) e^{j\Delta\theta} d\Delta\theta \\
&= \frac{4}{\pi^2}.
\end{aligned} \tag{36}$$

Therefore, $\mathbb{E}_{\mathbf{v}_{E,k}}(\text{conj}(\mathbf{v}_{E,k})\mathbf{v}_{E,k}^T)$ will be

$$\begin{aligned}
&\mathbb{E}_{\mathbf{v}_{E,k}}(\text{conj}(\mathbf{v}_{E,k})\mathbf{v}_{E,k}^T) = \\
&\begin{bmatrix} 1 & \mathbb{E}_{\Delta\theta_{2,1}}(e^{j(\Delta\theta_{2,1})}) & \dots & \mathbb{E}_{\Delta\theta_{M,1}}(e^{j(\Delta\theta_{M,1})}) \\ \mathbb{E}_{\Delta\theta_{1,2}}(e^{j(\Delta\theta_{1,2})}) & 1 & \dots & \mathbb{E}_{\Delta\theta_{M,2}}(e^{j(\Delta\theta_{M,2})}) \\ \vdots & \vdots & \ddots & \vdots \\ \mathbb{E}_{\Delta\theta_{1,M}}(e^{j(\Delta\theta_{1,M})}) & \mathbb{E}_{\Delta\theta_{2,M}}(e^{j(\Delta\theta_{2,M})}) & \dots & 1 \end{bmatrix} \\
&= \begin{bmatrix} 1 & \frac{4}{\pi^2} & \dots & \frac{4}{\pi^2} \\ \frac{4}{\pi^2} & 1 & \dots & \frac{4}{\pi^2} \\ \vdots & \vdots & \ddots & \vdots \\ \frac{4}{\pi^2} & \frac{4}{\pi^2} & \dots & 1 \end{bmatrix} = \mathbf{R}.
\end{aligned} \tag{37}$$

Next, we will derive $\mathbb{E}_{\theta_{E,k,j}}(e^{j\theta_{E,k,j}})$ and $\mathbb{E}_{\theta_{E,k,j}}(e^{-j\theta_{E,k,j}})$ as follows.

$$\begin{aligned}
&\mathbb{E}_{\theta_{E,k,j}}(e^{j\theta_{E,k,j}}) = \int_{-\frac{\pi}{2}}^{\frac{\pi}{2}} \frac{1}{\pi} e^{j\theta_{E,k,j}} d\theta_{E,k,j} \\
&= \int_{-\frac{\pi}{2}}^{\frac{\pi}{2}} \frac{1}{\pi} (\cos(\theta_{E,k,j}) + i\sin(\theta_{E,k,j})) d\theta_{E,k,j} \\
&= \int_{-\frac{\pi}{2}}^{\frac{\pi}{2}} \frac{1}{\pi} \cos(\theta_{E,k,j}) d\theta_{E,k,j} \\
&= \frac{2}{\pi}.
\end{aligned} \tag{38}$$

$$\begin{aligned}
&\mathbb{E}_{\theta_{E,k,j}}(e^{-j\theta_{E,k,j}}) = \int_{-\frac{\pi}{2}}^{\frac{\pi}{2}} \frac{1}{\pi} e^{-j\theta_{E,k,j}} d\theta_{E,k,j} \\
&= \int_{-\frac{\pi}{2}}^{\frac{\pi}{2}} \frac{1}{\pi} (\cos(\theta_{E,k,j}) - i\sin(\theta_{E,k,j})) d\theta_{E,k,j} \\
&= \int_{-\frac{\pi}{2}}^{\frac{\pi}{2}} \frac{1}{\pi} \cos(\theta_{E,k,j}) d\theta_{E,k,j} \\
&= \frac{2}{\pi}.
\end{aligned} \tag{39}$$

Thus, we have the following results

$$\begin{aligned}
&\mathbb{E}_{\mathbf{v}_{E,k}}(\text{conj}(\mathbf{v}_{E,k})) = [\mathbb{E}_{\theta_{E,k,1}}(e^{-j\theta_{E,k,1}}), \mathbb{E}_{\theta_{E,k,2}}(e^{-j\theta_{E,k,2}}), \\
&\dots, \mathbb{E}_{\theta_{E,k,M}}(e^{-j\theta_{E,k,M}})]^T = \frac{2}{\pi}\mathbf{1}.
\end{aligned} \tag{40}$$

$$\begin{aligned}
&\mathbb{E}_{\mathbf{v}_{E,k}}(\mathbf{v}_{E,k}^T) = [\mathbb{E}_{\theta_{E,k,1}}(e^{j\theta_{E,k,1}}), \mathbb{E}_{\theta_{E,k,2}}(e^{j\theta_{E,k,2}}), \\
&\dots, \mathbb{E}_{\theta_{E,k,M}}(e^{j\theta_{E,k,M}})] = \frac{2}{\pi}\mathbf{1}^T.
\end{aligned} \tag{41}$$

Therefore, we can derive $\hat{a}_k$ and $\hat{b}_k$ described in (8)-(9) according to (37), (40) and (41).

Appendix B

Benchmark Methods

1) Without phase errors: In this scheme, it considers an ideal scenario without phase errors at the IRS. Therefore, the corresponding optimization problem will be

$$\underset{\{\tau_k,\Gamma_k,P_{A,k},P_k\}}{\text{minimize}} \sum_{k=0}^{K} \tau_k \tag{42a}$$

$$\text{s.t.} \quad \tau_k \log_2\left(1 + \frac{P_k|\mathbf{g}_r^H\Gamma_k\mathbf{g}_{I,k} + g_{d,k}|^2}{\delta^2 + \gamma P_{A,k}}\right) \geq R_{k,\min}, \forall k \in \mathcal{K}, \tag{42b}$$

$$P_k\tau_k \leq \eta_k \sum_{i=0}^{k-1} P_{A,i}\tau_i|\mathbf{h}_{I,k}^H\Gamma_i\mathbf{h}_r + h_{d,k}|^2, \forall k \in \mathcal{K}, \tag{42c}$$

$$\text{C3-C5}. \tag{42d}$$

2) Without IRS: In this scheme, the HAP transmits the downlink energy signals to WDs and receives the uplink information from WDs without the aid of IRS. Hence, the corresponding optimization problem is given by

$$\underset{\{\tau_k,P_{A,k},P_k\}}{\text{minimize}} \sum_{k=0}^{K} \tau_k \tag{43a}$$

$$\text{s.t.} \quad \tau_k \log_2\left(1 + \frac{P_k|g_{d,k}|^2}{\delta^2 + \gamma P_{A,k}}\right) \geq R_{k,\min}, \forall k \in \mathcal{K}, \tag{43b}$$

$$P_k\tau_k \leq \eta_k \sum_{i=0}^{k-1} P_{A,i}\tau_i|h_{d,k}|^2, \forall k \in \mathcal{K}, \tag{43c}$$

$$\text{C4-C5}. \tag{43d}$$

This article has been accepted for publication in IEEE Internet of Things Journal. This is the author's version which has not been fully edited and content may change prior to final publication. Citation information: DOI 10.1109/JIOT.2022.3224533

3) Without energy causality: In this scheme, the k-th wireless device can utilize the harvested energy after τ_k for transmitting its uplink information, i.e., $E_{H,k} = \eta_k \sum_{i \neq k} P_{A,i}\tau_i|\mathbf{h}_{I,k}^H\Gamma_i\mathbf{h}_r + h_{d,k}|^2$. Therefore, the corresponding optimization problem can be formulated as

$$\underset{\{\tau_k,\hat{\Gamma}_k,P_{A,k},P_k\}}{\text{minimize}} \sum_{k=0}^{K} \tau_k \tag{44a}$$

$$\text{s.t.} \quad P_k\tau_k \leq \eta_k \sum_{i\neq k} P_{A,i}\tau_i|\mathbf{h}_{I,k}^H\hat{\Gamma}_i\mathbf{h}_r + h_{d,k}|^2, \quad \forall k \in \mathcal{K}, \tag{44b}$$

$$\text{C1, C3-C5.} \tag{44c}$$

A. Random phase shift

In this scheme, the phase shift $\{\Gamma_k\}$ of IRS is randomly generated from $(0, 2\pi]$, and the transmit power and time-slot variables are optimized by solving the following problem

$$\underset{\{\tau_k,P_{A,k},P_k\}}{\text{minimize}} \sum_{k=0}^{K} \tau_k \tag{45a}$$

$$\text{s.t.} \quad \tau_k \log_2\left(1 + \frac{P_k|\mathbf{g}_r^H\Gamma_k^*\Gamma_{E,k}\mathbf{g}_{I,k} + g_{d,k}|^2}{\delta^2 + \gamma P_{A,k}}\right) \geq R_{k,\min}, \forall k \in \mathcal{K}, \tag{45b}$$

$$P_k\tau_k \leq \eta_k \sum_{i=0}^{k-1} P_{A,i}\tau_i|\mathbf{h}_{I,k}^H\Gamma_i^*\Gamma_{E,i}\mathbf{h}_r + h_{d,k}|^2, \quad \forall k \in \mathcal{K}, \tag{45c}$$

$$\text{C4-C5.} \tag{45d}$$

References

[1] Y. Gao, Z. Qin, Z. Feng, Q. Zhang, O. Holland, and M. Dohler, "Scalable and reliable iot enabled by dynamic spectrum management for M2M in LTE-A," *IEEE Internet of Things Journal*, vol. 3, no. 6, pp. 1135–1145, 2016.

[2] J. Feng, L. Liu, Q. Pei, and K. Li, "Min-max cost optimization for efficient hierarchical federated learning in wireless edge networks," *IEEE Transactions on Parallel and Distributed Systems*, vol. 33, no. 11, pp. 2687–2700, 2022.

[3] L. Zhou, S. Leng, Q. Wang, and Q. Liu, "Integrated sensing and communication in UAV swarms for cooperative multiple targets tracking," *IEEE Transactions on Mobile Computing*, pp. 1–17, 2022.

[4] J. Feng, W. Zhang, Q. Pei, J. Wu, and X. Lin, "Heterogeneous computation and resource allocation for wireless powered federated edge learning systems," *IEEE Transactions on Communications*, vol. 70, no. 5, pp. 3220–3233, 2022.

[5] P. Ramezani and A. Jamalipour, "Toward the evolution of wireless powered communication networks for the future internet of things," *IEEE Network*, vol. 31, no. 6, pp. 62–69, 2017.

[6] S. Bi, Y. Zeng, and R. Zhang, "Wireless powered communication networks: An overview," *IEEE Wireless Communications*, vol. 23, no. 2, pp. 10–18, 2016.

[7] D. Niyato, D. I. Kim, M. Maso, and Z. Han, "Wireless powered communication networks: Research directions and technological approaches," *IEEE Wireless Communications*, vol. 24, no. 6, pp. 88–97, 2017.

[8] J. Hu, K. Yang, G. Wen, and L. Hanzo, "Integrated data and energy communication network: A comprehensive survey," *IEEE Communications Surveys and Tutorials*, vol. 20, no. 4, pp. 3169–3219, 2018.

[9] H. Kim, H. Lee, M. Ahn, H.-B. Kong, and I. Lee, "Joint subcarrier and power allocation methods in full duplex wireless powered communication networks for OFDM systems," *IEEE Transactions on Wireless Communications*, vol. 15, no. 7, pp. 4745–4753, 2016.

[10] S. Mao, L. Liu, N. Zhang, M. Dong, J. Zhao, J. Wu, and V. C. M. Leung, "Reconfigurable intelligent surface-assisted secure mobile edge computing networks," *IEEE Transactions on Vehicular Technology*, vol. 71, no. 6, pp. 6647–6660, 2022.

[11] C. Huang, S. Hu, G. C. Alexandropoulos, A. Zappone, C. Yuen, R. Zhang, M. D. Renzo, and M. Debbah, "Holographic mimo surfaces for 6G wireless networks: Opportunities, challenges, and trends," *IEEE Wireless Communications*, vol. 27, no. 5, pp. 118–125, 2020.

[12] C. Pan, H. Ren, K. Wang, M. Elkashlan, A. Nallanathan, J. Wang, and L. Hanzo, "Intelligent reflecting surface aided mimo broadcasting for simultaneous wireless information and power transfer," *IEEE Journal on Selected Areas in Communications*, vol. 38, no. 8, pp. 1719–1734, 2020.

[13] S. Mao, L. Liu, N. Zhang, J. Hu, K. Yang, F. R. Yu, and V. C. M. Leung, "Intelligent reflecting surface-assisted low-latency federated learning over wireless networks," *IEEE Internet of Things Journal*, pp. 1–1, 2022.

[14] M. Di Renzo, A. Zappone, M. Debbah, M.-S. Alouini, C. Yuen, J. de Rosny, and S. Tretyakov, "Smart radio environments empowered by reconfigurable intelligent surfaces: How it works, state of research, and the road ahead," *IEEE Journal on Selected Areas in Communications*, vol. 38, no. 11, pp. 2450–2525, 2020.

[15] Y. Liu, X. Liu, X. Mu, T. Hou, J. Xu, M. Di Renzo, and N. Al-Dhahir, "Reconfigurable intelligent surfaces: Principles and opportunities," *IEEE Communications Surveys and Tutorials*, vol. 23, no. 3, pp. 1546–1577, 2021.

[16] S. Mao, S. Leng, J. Hu, and K. Yang, "Energy-efficient transmission schemes for cooperative wireless powered cellular networks," *IEEE Transactions on Green Communications and Networking*, vol. 3, no. 2, pp. 494–504, 2019.

[17] S. Mao, K. Yang, J. Hu, D. Li, D. Lan, M. Xiao, and Y. Xiong, "Intelligent reflecting surface-aided wireless powered hybrid backscatter-active communication networks," *IEEE Transactions on Vehicular Technology*, pp. 1–6, 2022.

[18] H. Ju and R. Zhang, "Throughput maximization in wireless powered communication networks," *IEEE Transactions on Wireless Communications*, vol. 13, no. 1, pp. 418–428, 2014.

[19] Q. Wu, M. Tao, D. W. Kwan Ng, W. Chen, and R. Schober, "Energy-efficient resource allocation for wireless powered communication networks," *IEEE Transactions on Wireless Communications*, vol. 15, no. 3, pp. 2312–2327, 2016.

[20] H. Lee, K.-J. Lee, H. Kim, B. Clerckx, and I. Lee, "Resource allocation techniques for wireless powered communication networks with energy storage constraint," *IEEE Transactions on Wireless Communications*, vol. 15, no. 4, pp. 2619–2628, 2016.

[21] K. Xiong, C. Chen, G. Qu, P. Fan, and K. B. Letaief, "Group cooperation with optimal resource allocation in wireless powered communication networks," *IEEE Transactions on Wireless Communications*, vol. 16, no. 6, pp. 3840–3853, 2017.

[22] E. Boshkovska, D. W. K. Ng, N. Zlatanov, A. Koelpin, and R. Schober, "Robust resource allocation for MIMO wireless powered communication networks based on a non-linear EH model," *IEEE Transactions on Communications*, vol. 65, no. 5, pp. 1984–1999, 2017.

[23] L. Xie, J. Xu, and R. Zhang, "Throughput maximization for UAV-enabled wireless powered communication networks," *IEEE Internet of Things Journal*, vol. 6, no. 2, pp. 1690–1703, 2019.

[24] K. E. Kolodziej, B. T. Perry, and J. S. Herd, "In-band full-duplex technology: Techniques and systems survey," *IEEE Transactions on Microwave Theory and Techniques*, vol. 67, no. 7, pp. 3025–3041, 2019.

[25] H. Ju and R. Zhang, "Optimal resource allocation in full-duplex wireless-powered communication network," *IEEE Transactions on Communications*, vol. 62, no. 10, pp. 3528–3540, 2014.

[26] X. Kang, C. K. Ho, and S. Sun, "Full-duplex wireless-powered communication network with energy causality," *IEEE Transactions on Wireless Communications*, vol. 14, no. 10, pp. 5539–5551, 2015.

[27] R. Rezaei, S. Sun, X. Kang, Y. L. Guan, and M. R. Pakravan, "Secrecy throughput maximization for full-duplex wireless powered IoT networks under fairness constraints," *IEEE Internet of Things Journal*, vol. 6, no. 4, pp. 6964–6976, 2019.

[28] M. S. Iqbal, Y. Sadi, and S. Coleri, "Minimum length scheduling for full duplex time-critical wireless powered communication networks," *IEEE Transactions on Wireless Communications*, vol. 19, no. 9, pp. 5993–6006, 2020.

This article has been accepted for publication in IEEE Internet of Things Journal. This is the author's version which has not been fully edited and content may change prior to final publication. Citation information: DOI 10.1109/JIOT.2022.3224533

[29] ——, "Minimum length scheduling for discrete-rate full-duplex wireless powered communication networks," *IEEE Transactions on Wireless Communications*, vol. 21, no. 1, pp. 135–148, 2022.
[30] D. K. P. Asiedu, S. Mahama, C. Song, D. Kim, and K.-J. Lee, "Beamforming and resource allocation for multiuser full-duplex wireless-powered communications in IoT networks," *IEEE Internet of Things Journal*, vol. 7, no. 12, pp. 11 355–11 370, 2020.
[31] Q. Wu, X. Guan, and R. Zhang, "Intelligent reflecting surface-aided wireless energy and information transmission: An overview," *Proceedings of the IEEE*, vol. 110, no. 1, pp. 150–170, 2022.
[32] S. Mao, N. Zhang, L. Liu, J. Wu, M. Dong, K. Ota, T. Liu, and D. Wu, "Computation rate maximization for intelligent reflecting surface enhanced wireless powered mobile edge computing networks," *IEEE Transactions on Vehicular Technology*, vol. 70, no. 10, pp. 10 820–10 831, 2021.
[33] Q. Wu and R. Zhang, "Weighted sum power maximization for intelligent reflecting surface aided SWIPT," *IEEE Wireless Communications Letters*, vol. 9, no. 5, pp. 586–590, 2020.
[34] Y. Zheng, S. Bi, Y.-J. A. Zhang, X. Lin, and H. Wang, "Joint beamforming and power control for throughput maximization in IRS-assisted MISO WPCNs," *IEEE Internet of Things Journal*, vol. 8, no. 10, pp. 8399–8410, 2021.
[35] Z. Chu, P. Xiao, D. Mi, W. Hao, M. Khalily, and L.-L. Yang, "A novel transmission policy for intelligent reflecting surface assisted wireless powered sensor networks," *IEEE Journal of Selected Topics in Signal Processing*, vol. 15, no. 5, pp. 1143–1158, 2021.
[36] Y. Xu, Z. Gao, Z. Wang, C. Huang, Z. Yang, and C. Yuen, "RIS-enhanced WPCNs: Joint radio resource allocation and passive beamforming optimization," *IEEE Transactions on Vehicular Technology*, vol. 70, no. 8, pp. 7980–7991, 2021.
[37] Z. Li, W. Chen, Q. Wu, H. Cao, K. Wang, and J. Li, "Robust beamforming design and time allocation for IRS-assisted wireless powered communication networks," *IEEE Transactions on Communications*, vol. 70, no. 4, pp. 2838–2852, 2022.
[38] B. Lyu, P. Ramezani, D. T. Hoang, S. Gong, Z. Yang, and A. Jamalipour, "Optimized energy and information relaying in self-sustainable IRS-empowered WPCN," *IEEE Transactions on Communications*, vol. 69, no. 1, pp. 619–633, Jan. 2021.
[39] M. Hua and Q. Wu, "Joint dynamic passive beamforming and resource allocation for IRS-aided full-duplex WPCN," *IEEE Transactions on Wireless Communications*, vol. 21, no. 7, pp. 4829–4843, 2022.
[40] D. Li, "Ergodic capacity of intelligent reflecting surface-assisted communication systems with phase errors," *IEEE Communications Letters*, vol. 24, no. 8, pp. 1646–1650, 2020.
[41] Z. Chu, J. Zhong, P. Xiao, D. Mi, W. Hao, R. Tafazolli, and A. Feresidis, "RIS assisted wireless powered IoT networks with phase shift error and transceiver hardware impairment," *IEEE Transactions on Communications*, vol. 70, no. 7, pp. 4910–4924, 2022.
[42] Q. Wu and R. Zhang, "Towards smart and reconfigurable environment: Intelligent reflecting surface aided wireless network," *IEEE Communications Magazine*, vol. 58, no. 1, pp. 106–112, Jan. 2020.
[43] Z. Xing, R. Wang, J. Wu, and E. Liu, "Achievable rate analysis and phase shift optimization on intelligent reflecting surface with hardware impairments," *IEEE Transactions on Wireless Communications*, vol. 20, no. 9, pp. 5514–5530, 2021.
[44] Q. Wu, Y. Zeng, and R. Zhang, "Joint trajectory and communication design for multi-UAV enabled wireless networks," *IEEE Transactions on Wireless Communications*, vol. 17, no. 3, pp. 2109–2121, 2018.

Sun Mao received the Ph.D. degree in communication and information systems from the University of Electronic Science and Technology of China, Chengdu, China, in 2020. From 2018 to 2019, he was with University of Oslo, Oslo, Norway, as a visiting Ph.D student. He is currently a Lecturer with the College of Computer Science, Sichuan Normal University. His research interests include simultaneous wireless information and power transfer, mobile edge computing, and intelligent reflecting surface-assisted wireless networks.

Lei Liu received the B.Eng. degree in electronic information engineering from Zhengzhou University, Zhengzhou, China, in 2010, and the M.Sc. and Ph.D degrees in communication and information systems from Xidian University, Xian, China, in 2013 and 2019, respectively. From 2013 to 2015, he was employed by a subsidiary of China Electronics Corporation. From 2018 to 2019, he was supported by China Scholarship Council to be a visiting Ph.D. student with the University of Oslo, Oslo, Norway. He is currently a Lecturer with the State Key Laboratory of Integrated Service Networks, Xidian University, and also with the Xidian Guangzhou Institute of Technology. His research interests include vehicular ad hoc networks, intelligent transportation, mobile-edge computing, and Internet of Things.

Ning Zhang received the Ph.D. degree from the University of Waterloo, Canada, in 2015. He was a Post-Doctoral Research Fellow with the University of Waterloo and also with the University of Toronto, Canada. He is currently an Associate Professor with the University of Windsor, Canada. He received the Best Paper Awards from IEEE Globecom in 2014, IEEE WCSP in 2015, and the Journal of Communications and Information Networks in 2018, IEEE ICC in 2019, the IEEE Technical Committee on Transmission Access and Optical Systems in 2019, and IEEE ICCC in 2019, respectively. He also serves/served as a track chair for several international conferences and a co-chair for several international workshops. He serves as an Associate Editor for the IEEE Internet of Things Journal, the IEEE Transactions on Cognitive Communications and Networking, IEEE Access, IET Communications, and Vehicular Communications. He was a Guest Editor of several international journals, such as the IEEE Wireless Communications, the IEEE Transactions on Industrial Informatics, and the IEEE Transactions on Cognitive Communications and Networking.

Jie Hu received his B.Eng. and M.Sc. degrees from Beijing University of Posts and Telecommunications, China, in 2008 and 2011, respectively, and received the Ph.D. degree from the School of Electronics and Computer Science, University of Southampton, U.K., in 2015. Since March 2016, he has been working with the School of Information and Communication Engineering, University of Electronic Science and Technology of China (UESTC), China. He is now a Research Professor. He has been elected into UESTCs Fundamental Research Program for Young Scientists since 2018. He also won UESTCs Academic Young Talent Award in 2019. Now he is supported by the "100 Talents" program of UESTC. His research now is mainly funded by National Natural Science Foundation of China (NSFC). He is an editor for both IEEE Wireless Communications Letters and IET Smart Cities. He serves for IEEE Communications Magazine, IEEE/CIC China Communications, Frontiers in Communications and Networks as well as ZTE communications as a guest editor. He is a program vice-chair for IEEE TrustCom 2020 and a technical program committee (TPC) chair for IEEE UCET 2021. He also serves as a TPC member for several prestigious IEEE conferences, such as IEEE Globecom/ICC/WCSP and etc. He has won the best paper award of IEEE SustainCom 2020. His current research focuses on wireless communications and resource management for 6G, wireless information and power transfer as well as integrated communication, computing and sensing.

This article has been accepted for publication in IEEE Internet of Things Journal. This is the author's version which has not been fully edited and content may change prior to final publication. Citation information: DOI 10.1109/JIOT.2022.3224533

Kun Yang received his PhD from the Department of Electronic and Electrical Engineering of University College London (UCL), UK. He is currently a Chair Professor in the School of Computer Science and Electronic Engineering, University of Essex, leading the Network Convergence Laboratory (NCL), UK. He is also an affiliated professor at UESTC, China. Before joining in the University of Essex at 2003, he worked at UCL on several European Union (EU) research projects for several years. His main research interests include wireless networks and communications, IoT networking, data and energy integrated networks and mobile computing. He manages research projects funded by various sources such as UK EPSRC, EU FP7/H2020 and industries. He has published 300+ papers and filed 20 patents. He serves on the editorial boards of both IEEE (e.g., IEEE TNSE, IEEE ComMag, IEEE WCL) and non-IEEE journals. He is a Member of Academia Europaea (MAE). He is a Senior Member of IEEE (since 2008), a Fellow of IET and a Fellow of BCS. He is an IEEE ComSoc Distinguished Lecturer (2020-2021).

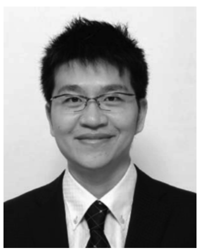

Mianxiong Dong received the B.S., M.S., and Ph.D. degrees in computer science and engineering from the University of Aizu, Japan. He became the youngest ever Professor with the Muroran Institute of Technology, Japan, where he currently serves as the Vice President. He was a JSPS Research Fellow with the School of Computer Science and Engineering, The University of Aizu, and was a Visiting Scholar with BBCR Group, University of Waterloo, Canada, supported by JSPS Excellent Young Researcher Overseas Visit Program from April 2010 to August 2011. He is the recipient of the IEEE TCSC Early Career Award 2016, the IEEE SCSTC Outstanding Young Researcher Award 2017, the 12th IEEE ComSoc AsiaPacific Young Researcher Award 2017, the Funai Research Award 2018, and the NISTEP Researcher 2018 (one of only 11 people in Japan) in recognition of significant contributions in science and technology. He has been serving as the Vice Chair of IEEE Communications Society Asia/Pacific Region Information Services Committee and Meetings and Conference Committee, a Leading Symposium Chair of IEEE ICC 2019, a Student Travel Grants Chair of IEEE GLOBECOM 2019, and a Symposium Chair of IEEE GLOBECOM in 2016 and 2017. He is currently the Member of Board of Governors and the Chair of Student Fellowship Committee of IEEE Vehicular Technology Society, and a Treasurer of IEEE ComSoc Japan Joint Sections Chapter. He is Clarivate Analytics 2019 Highly Cited Researcher (Web of Science).

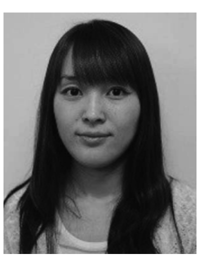

Kaoru Ota received the B.S. degree in computer science and engineering from the University of Aizu, Japan, in 2006, the M.S. degree in computer science from Oklahoma State University, USA, in 2008, and the Ph.D. degree in computer science and engineering from the University of Aizu in 2012. She is currently an Associate Professor with the Department of Sciences and Informatics, Muroran Institute of Technology, Japan. From March 2010 to March 2011, she was a Visiting Scholar with the University of Waterloo, Canada. She is an Editor of IEEE Transactions on Vehicular Technology (TVT), IEEE Internet of Things Journal, IEEE Communications Letters, Peer-to-Peer Networking and Applications (Springer), Ad Hoc and Sensor Wireless Networks, International Journal of Embedded Systems (Inderscience), and Smart Technologies for Emergency Response and Disaster Management (IGI Global), and a Guest Editor of ACM Transactions on Multimedia Computing, Communications and Applications (leading), IEEE Internet of Things Journal, IEEE Communications Magazine, IEEE Network, IEEE Wireless Communications, IEEE Access, IEICE Transactions on Information and Systems, and Ad Hoc and Sensor Wireless Networks (Old City Publishing).